

Cell Reports, Volume 31

Supplemental Information

Identification of a G-Protein-Independent

Activator of GIRK Channels

Yulin Zhao, Peter Man-Un Ung, Gergely Zahoránszky-Kóhalmi, Alexey V. Zakharov, Natalia J. Martinez, Anton Simeonov, Ian W. Glaaser, Ganesha Rai, Avner Schlessinger, Juan J. Marugan, and Paul A. Slesinger



Figure S1. Sequence alignment for the three major domains of the alcohol pocket in GIRK1/GIRK2 channels Related to Figures 3 and 5. Amino acid mutations indicated for GIRK1 (orange) and GIRK2 (blue). Boxed residues indicate alcohol-sensitive site identified previously (Aryal et al., 2009). Cartoon shows one view of the alcohol pocket in a GIRK1/GIRK2 heterotetrameric channel.

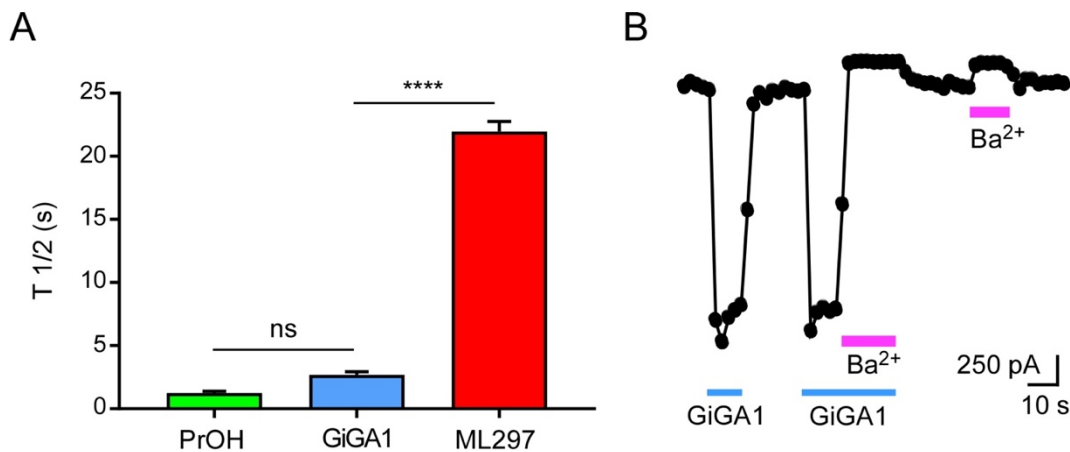


Figure S2. GiGA1 deactivation rates and inhibition by Ba²⁺. Related to Figure 2. (A) Bar graph shows mean deactivation rate ($T_{1/2}$) following ProOH (100 mM), GiGA1 (100 μ M), and ML297 (10 μ M)-induced activation of GIRK1/GIRK2 heterotetramers. **** $P < 0.0001$ for GiGA1 vs. ML297; One-way ANOVA: Bonferroni's Multiple Comparison post hoc test ($F(2, 27) = 555.3; P < 0.0001$) ($n=10$). ns: not significant. Error bars represent S.E.M.. (B) Trace show the current response to GiGA1 (100 μ M), and/or Ba²⁺ (1 mM) for GIRK1/GIRK2 channels.

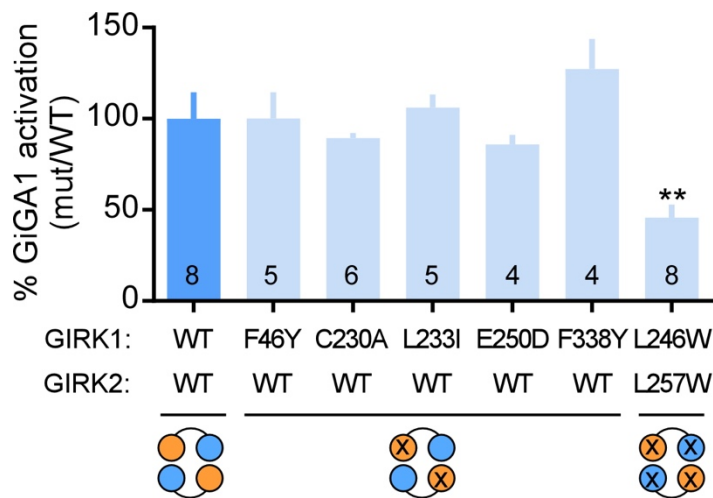


Figure S3. Percentage GiGA1 activation for mutants. Related to Figures 3 and 5. Bar graph shows the mean response of wild-type and mutant GIRK1/GIRK2 channels with GiGA1, normalized to the ML297-induced current. ** $P = 0.0017$ vs. GIRK1/GIRK2 WT; One-way ANOVA: Bonferroni's Multiple Comparison Test ($F(6, 28) = 8.477$; $P < 0.0001$). n indicated on graph. Error bars represent S.E.M..

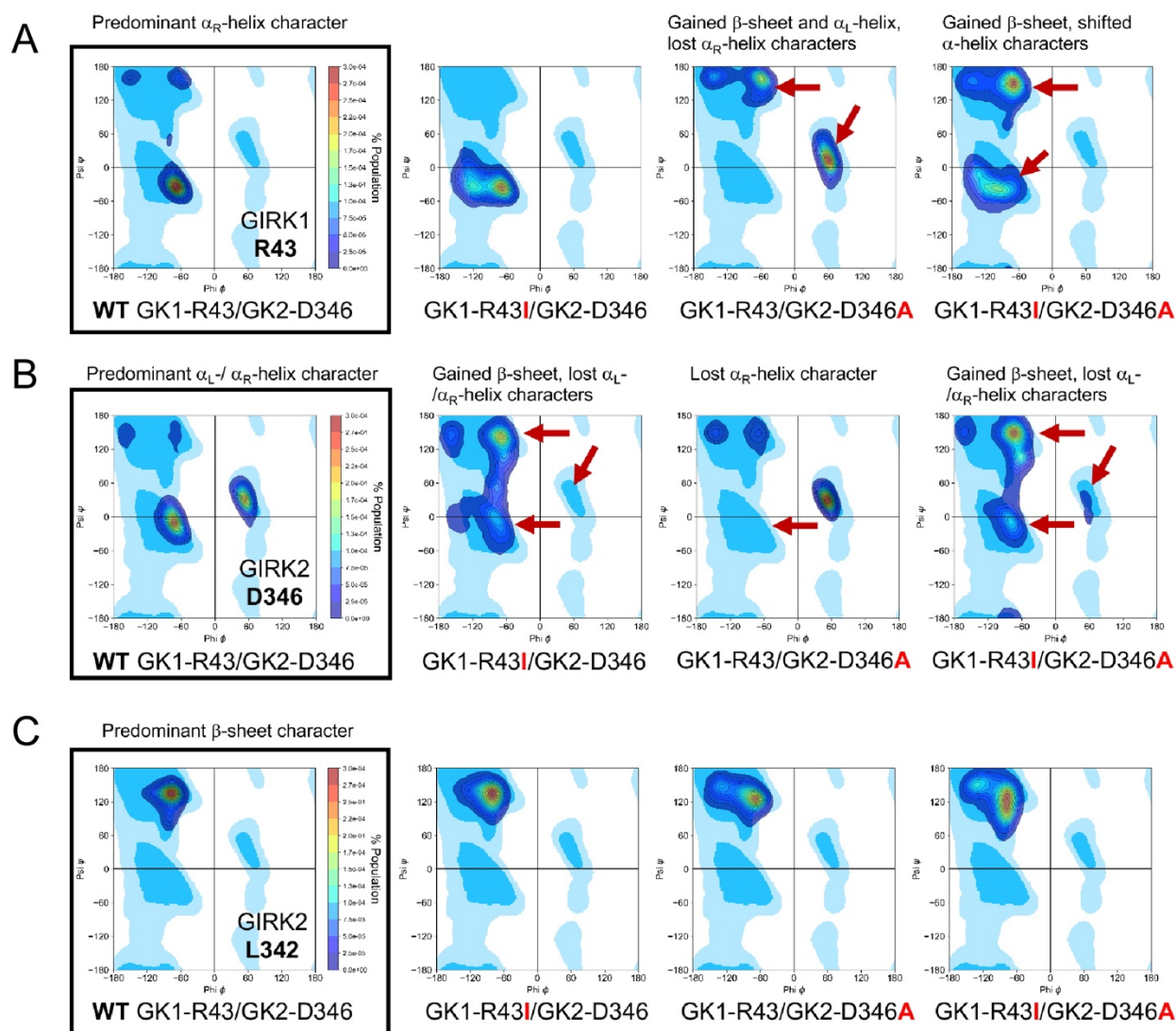


Figure S4. Molecular dynamics simulations of wild-type and mutant GIRK1/GIRK2 heterotetramer. Related to Figures 2, 3 and 5. Ramachandran plots of the mutated residues and a residue in the vicinity of mutations using Gaussian accelerated Molecular Dynamics (GaMD) simulations of GIRK1/GIRK2 heterotetramers. Distribution of the residue backbone dihedral angles is depicted as contoured density plot, in which the density is shown as a continuum of high to low in red to blue color, respectively. Known dihedral angle distribution of common amino acids is shown in the background as reference (light cyan and cyan area). **(A, B)** Single-mutation of GIRK1_{R43I} or GIRK2_{D346A} has slight effect on distribution of its own backbone dihedral angles (secondary structures). However, GIRK1_{R43I} single-mutation affects the distribution of secondary structures of GIRK2_{D346} and vice versa. Double-mutation has an additive effect on the backbone dihedral angles. **(C)** While GIRK2_{L342} is in the alcohol pocket and in the vicinity of the mutated residues, its secondary structure distribution in the simulation was unaffected by the mutations.

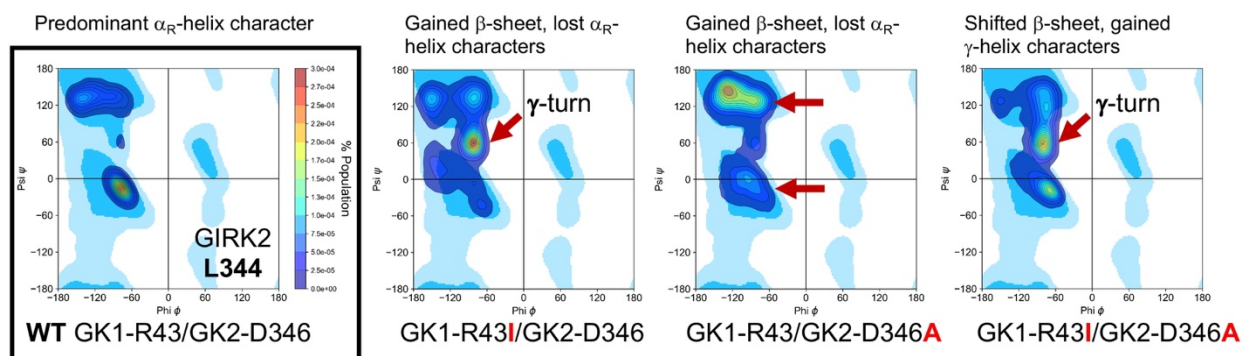


Figure S5. Molecular dynamics simulations of wild-type and mutant GIRK1/GIRK2 heterotetramers. Related to Figure 5. Ramachandran plots of GIRK2_{L344} in the presence of mutations in GaMD simulations of GIRK1/GIRK2 heterotetramers. Single- and double-mutations of GIRK1_{R43I} and GIRK2_{D346A} affect the distribution of GIRK2_{L344} secondary structures: GIRK2_{L344} lost the right-handed α_R -helix character while gaining β -sheet and inverted γ -turn characters.

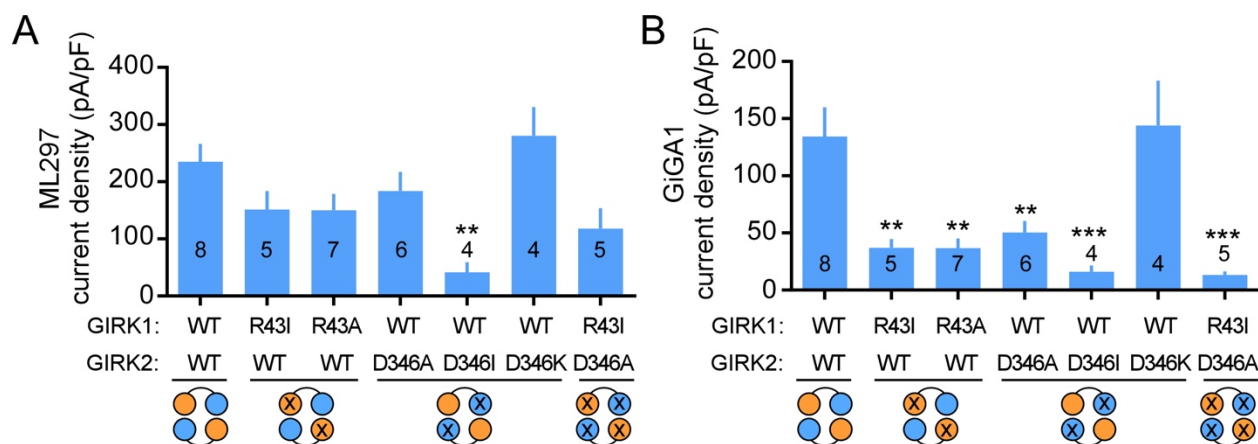


Figure S6. Current density for ML297- and GiGA1-activated currents. Related to Figure 5. Bar graphs show the mean current density for ML297 (A) and GiGA1 (B) induced responses for wild-type and mutant GIRK1/GIRK2 channels. (A) ** $P = 0.0025$ vs. GIRK1/GIRK2 WT; One-way ANOVA: Bonferroni's Multiple Comparison Test ($F(6, 32) = 4.354; P=0.0025$). (B) ** $P < 0.01$, *** $P < 0.001$ vs. GIRK1/GIRK2 WT; One-way ANOVA: Bonferroni's Multiple Comparison Test ($F(6, 32) = 8.244; P < 0.0001$). n indicated on graph. Error bars represent S.E.M.

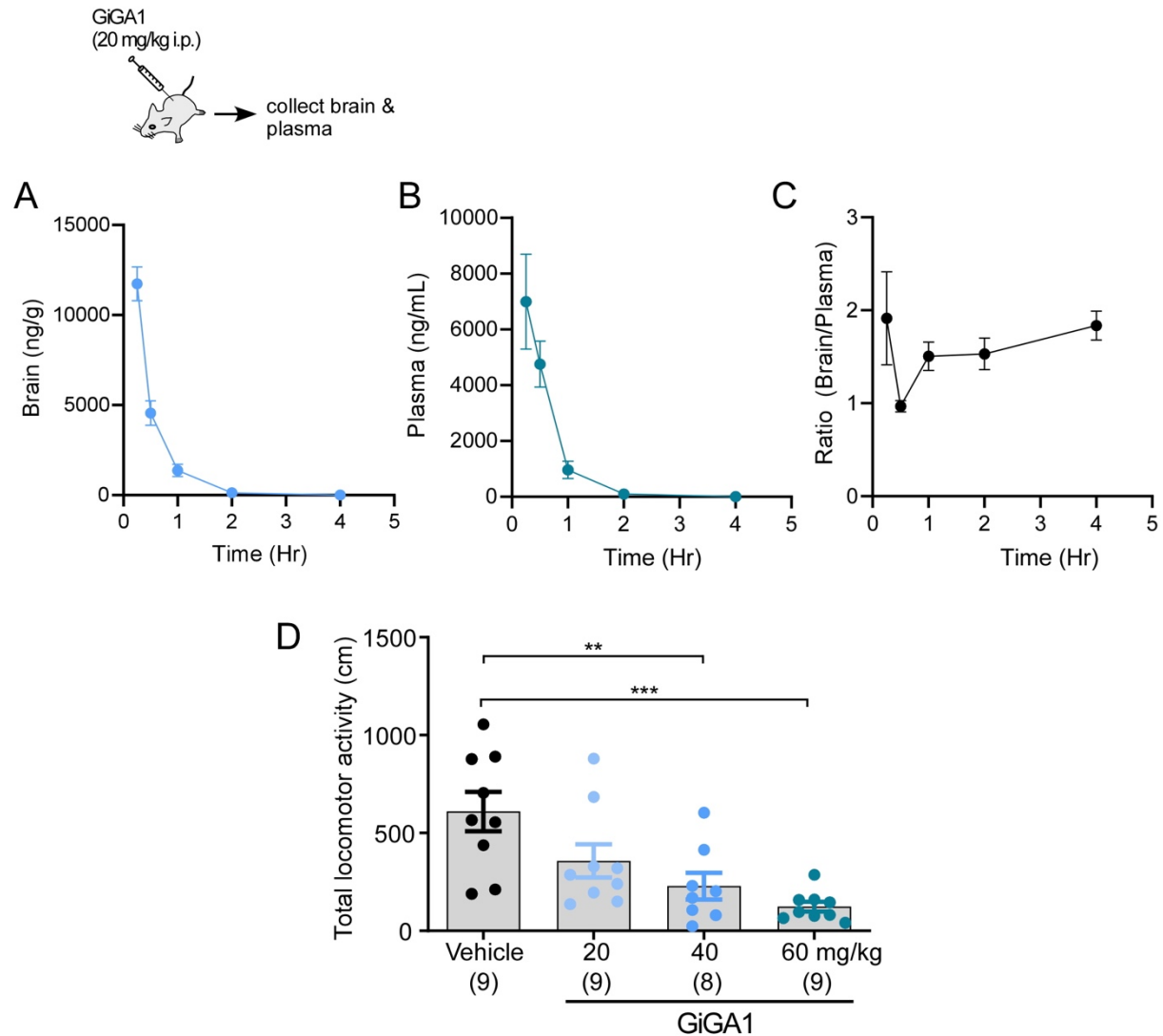


Figure S7. In vivo PK and effect on motor activity for GiGA1. Related to Figure 7 and STAR methods. (A-C) Pharmacokinetic (PK) profiles for GiGA1 *in vivo*. Levels of GiGA1 were measured in brain (A) and plasma (B) using LC/MS/MS, and are plotted against time after i.p. injection (n=3 mice per point). (C) Brain to plasma ratio is calculated over time. Note that GiGA1 has high brain permeability. (D) Bar graph shows total distance mice traveled 5 min after injection of vehicle or the indicated doses of GiGA1. ** $P = 0.0042$, *** $P = 0.0002$ vs. Vehicle; One-way ANOVA: Bonferroni's Multiple Comparison Test ($F(3, 31) = 7.856$; $P = 0.0005$). n indicated on graph. Error bars represent S.E.M..

Table S1: List of chemical compounds

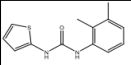
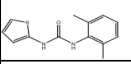
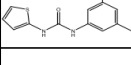
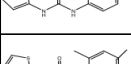
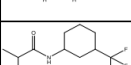
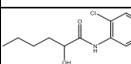
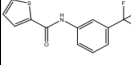
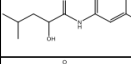
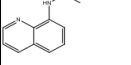
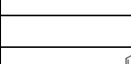
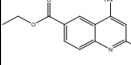
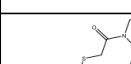
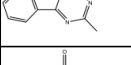
Name	NCATS ID	Chemical Name	
NCATS_1	proprietary		
NCATS_2	NCGC00113365-01		1-(2,3-dimethylphenyl)-3-(thiophen-2-yl)urea
NCATS_2.1	MLS000093627		1-(2,6-dimethylphenyl)-3-(thiophen-2-yl)urea
NCATS_2.2	NCGC00113368		1-(3,5-dimethylphenyl)-3-(thiophen-2-yl)urea
NCATS_2.3 / GIGA1	NCGC00092666		1-(2-methylphenyl)-3-(thiophen-2-yl)urea
NCATS_2.4	NCGC00113341		1-(2,4-dimethylphenyl)-3-(thiophen-2-yl)urea
NCATS_3	NCGC00262920-01		N-(3-(trifluoromethyl)cyclohexyl)isobutyramide
NCATS_4	NCGC00168723-01		N-(2-chloro-5-(trifluoromethyl)phenyl)-2-hydroxyhexanamide
NCATS_5	NCGC00229669-01		N-(3-(trifluoromethyl)phenyl)thiophene-2-carboxamide
NCATS_6	NCGC00168728-01		N-(2-chloro-5-(trifluoromethyl)phenyl)-2-hydroxy-4-methylpentanamide
NCATS_7	NCGC00161731-01		N-(quinolin-8-yl)acetamide
NCATS_8	proprietary		
NCATS_9	proprietary		
NCATS_10	NCGC00099858-01		3-((6-(ethoxycarbonyl)-2-methylquinolin-4-yl)amino)benzoic acid
NCATS_11	proprietary		
NCATS_12	MLS000041587-02		1-(3,4-dihydroquinolin-1(2H)-yl)-2-((2-methylbenzofuro[3,2-d]pyrimidin-4-yl)thio)ethan-1-one
NCATS_13	MLS001005104-02		2-((5-amino-1H-1,2,4-triazol-3-yl)thio)-N-(1,2,3,4-tetrahydronaphthalen-1-yl)acetamide

Table S1: List of chemical compounds and their structures screened in this study. Related to Figures 1E and 2A.